Army Research Laboratory

Confocal Microscopy Studies for Plasma Surface Modified Films and Fibers

by Donovan Harris and Daphne Pappas

ARL-TR-4004 **December 2006**

NOTICES

Disclaimers

Army Research Laboratory
Aberdeen Proving Ground, MD 21005-5069

ARL-TR-4004 **December 2006**

Confocal Microscopy Studies for Plasma Surface Modified Films and Fibers

Donovan Harris and Daphne Pappas
Weapons and Materials Research Directorate, ARL

REPORT DOCUMENTATION PAGE

Form Approved
OMB No. 0704-0188

1. REPORT DATE *(DD-MM-YYYY)* December 2006	**2. REPORT TYPE** Interim	**3. DATES COVERED (From - To)** October 2005–May 2006

4. TITLE AND SUBTITLE
Confocal Microscopy Studies for Plasma Surface Modified Films and Fibers

5a. CONTRACT NUMBER

5b. GRANT NUMBER

5c. PROGRAM ELEMENT NUMBER

6. AUTHOR(S)
Donovan Harris and Daphne Pappas

5d. PROJECT NUMBER
AH84

5e. TASK NUMBER

5f. WORK UNIT NUMBER

7. PERFORMING ORGANIZATION NAME(S) AND ADDRESS(ES)
U.S. Army Research Laboratory
ATTN: AMSRD-ARL-WM-MA
Aberdeen Proving Ground, MD 21005-5069

8. PERFORMING ORGANIZATION REPORT NUMBER
ARL-TR-4004

9. SPONSORING/MONITORING AGENCY NAME(S) AND ADDRESS(ES)

10. SPONSOR/MONITOR'S ACRONYM(S)

11. SPONSOR/MONITOR'S REPORT NUMBER(S)

12. DISTRIBUTION/AVAILABILITY STATEMENT
Approved for public release; distribution is unlimited.

13. SUPPLEMENTARY NOTES

14. ABSTRACT

The focus of this work is plasma-treated Nylon 6 films and woven fabrics characterization by a confocal laser scanning microscope. The purposes of these efforts were the preliminary characterization of vendor-treated materials prior to equipment installation and the evaluation of instrumentation capability to provide the data required in a time-effective manner. Brief technical discussions of the atmospheric plasma process and some of the resultant surface chemistries are presented in conjunction with the observed topological changes and related characterization issues.

Results reveal that after exposure to helium nitrogen and helium acetylene plasmas under atmospheric pressure, polymer surface modification is achieved and carbonyl and hydroxyl groups are grafted. Moreover, the surface morphology changes, and rougher surfaces are created. These effects result in enhancement of the surface energy of the treated polymers and therefore can be used in composite systems with success. The work proves that there is a need for better correlation between the atomic force microscopy and the confocal laser scanning microscopy when working with similar materials and processes.

15. SUBJECT TERMS
atmospheric plasma processing, roughness measurements

16. SECURITY CLASSIFICATION OF:			**17. LIMITATION OF ABSTRACT**	**18. NUMBER OF PAGES**	**19a. NAME OF RESPONSIBLE PERSON** Donovan Harris
a. REPORT UNCLASSIFIED	**b. ABSTRACT** UNCLASSIFIED	**c. THIS PAGE** UNCLASSIFIED	UL	28	**19b. TELEPHONE NUMBER** (*Include area code*) 410-306-0707

Standard Form 298 (Rev. 8/98)
Prescribed by ANSI Std. Z39.18

Contents

List of Figures

List of Tables

Acknowledgments

This research was supported in part by an appointment to the Research Participation Program at the U.S. Army Research Laboratory (ARL) administered by the Oak Ridge Institute for Science and Education through an interagency agreement between the U.S. Department of Energy and ARL.

1. Introduction

This report addresses the analyses of a surface roughness done in preparation for the installation of two atmospheric pressure plasma systems. The studied surfaces were Spectra[*] fabric and Nylon 6 fibers and films, plasma treated under atmospheric pressure conditions. The plasma exposure results in chemical modification and activation of the surface and interesting morphological changes. In our case, He-N_2 was utilized, and an increase of the surface roughness was expected. The roughness measurements were performed using contact and noncontact instrumentation—atomic force microscopy (AFM) and confocal microscopy. The report describes instrumental and sample preparation issues affecting the test data and roughness analysis. These methods, when coupled with surface analytical tools like x-ray photoelectron spectroscopy and water contact angle measurements, can give a complete picture of the plasma-surface interactions occurring during the treatment of the polymeric material and are therefore particularly interesting.

2. Background

High-strength organic fibers including polyaramid, polyamide, and polypropylene are used as reinforcements in polymer composite materials. However, their more widespread use is limited by poor interfacial adhesion to some polymer matrix materials, relative low thermal resistance, and low mechanical strength. Fiber-matrix adhesion in advanced composites depends on the physical and chemical interactions at their interface. The adhesion between the fabric and other materials such as epoxies, other polymers, and metals can be improved by grafting new chemical groups on the surfaces that will act as bridges with the other material. Moreover an increased roughness of the surface through a process will increase the reactive area.[1] Compared to fabrics, polymer films also have poor adhesion properties but are easier to modify due to their geometric uniformity and can be used as model surfaces.

Plasma treatment of organic materials is a technique employed to modify their surfaces and enhance properties such as adhesive bonding, durability, wettability, biocompatibility, and adhesion of dyes.[2] One of the main advantages of the method is that it is a surface-oriented method—impact is profound at a shallow depth of the polymer surface, leaving the bulk practically unaffected. Plasma treatment is an alternative method to wet chemical treatments,

---

[*] Spectra is a registered trademark of Bally Ribbon Mills.

[1] Brown, J.; Mathys, Z. Plasma Surface Modification of Advanced Organic Fibres, Part V: Effects on the Mechanical Properties of Aramid/Phenolic Composites. *J. Mater. Sci.* **1997**, *32*, 2599.

[2] Wertheimer, M.; Fozza, A.; Hollander, A. Industrial Processing of Polymers by Low Pressure Plasmas. *Nucl. Instr. Meth. Phys. Res. B* **1999**, *151*, 65.

provides a uniform modification, is environmentally friendly, and requires short process times. The energetic electrons, ions, excited atoms, molecules, and UV photons present in the gas phase are responsible for the surface modification, but their role in the interaction with the polymer surfaces is yet not fully understood due to the complexity of the gas phase and the polymer structure. When a polymer surface is exposed to plasma, it is bombarded by the plasma active species just described and leads to chain scissions and polymer degradation. If a plasma reactive gas is used, the appearance of new functional groups on the surface is expected. Until recently, low-pressure glow discharges were used to perform the modification process, requiring complex vacuum equipment, limited sample size, and longer process times.

Atmospheric plasma systems are gaining popularity nowadays in order to scale up and make the method appealing to industrial applications. Throughput is high, reinforced by the high species flux obtained from high-pressure operation.

3. Experimental

In this work, polyamide (Nylon 6) and ultra high molecular weight polyethylene (Spectra) fibers and nylon films were treated under atmospheric pressure glow discharges. The effects on the morphology and chemistry of the material were also studied. The plasma-induced changes in surface chemistry, topology, and roughness were documented using x-ray photoelectron spectroscopy (XPS), field emission-environmental scanning electron microscope, AFM, and confocal laser scanning microscopy (LSM). The scope of this report is confined to the last two techniques, AFM and LSM, while wettability and XPS results are presented elsewhere.[3, 4]

The atmospheric plasma system used for the surface treatments was a Sigma Technologies large scale plasma system. The two electrodes of the system incorporate a porous metallic layer with pores of average size within one order of magnitude of the mean free path of the plasma gas at atmospheric pressure. The gases in this case, N_2-He and C_2H_2-He, were injected into the electrode at atmospheric pressure and allowed to diffuse through the porous layer, forming a uniform glow discharge. Helium is typically used to initiate and generate the plasma at atmospheric pressure before another gas is introduced to the system. The operating frequency was 90 kHz, with an operating power of 850 W.

The average diameter of Nylon 6 and Spectra fibers was 20 and 100 µm, respectively, and Nylon 6 films (Goodfellow) were 100 µm thick. The polymers were exposed to the plasma created between this electrode and a second electrode covered by a dielectric layer. All fabric

---

[3] Pappas, D.; Bujanda, A.; Demaree, J. D.; Hirvonen, J. K.; Kosik, W.; Jensen, R.; McKnight, S. Atmospheric Plasma Treatment of Polyamide Films. *Proceedings of the 49th SVC Ann. Techn. Conference*, Washington, DC, 22–27 April 2006.

[4] Pappas, D.; Bujanda, A.; Demaree, J. D.; Hirvonen, J. K.; Kosik, W.; Jensen, R.; McKnight, S. Surface Modification of Polyamide Fibers and Films Using Atmospheric Plasmas. Accepted to appear in *Surf. Coat. Technol*.

samples were cut into 7- × 25-mm rectangular pieces. Single fiber tests were not preferred because the extraction of a single fiber may have resulted in an uneven distribution of finishes, coatings, and sizing.

The plasma modified surfaces were subsequently treated with colloidal silica to increase surface roughness of the fibers. The colloidal silica particles were coupled to the modified surfaces using traditional organofunctional silane chemistry (3-glycidoxytrimethoxysilane, GPS).[5]

Surface roughness measurements were needed to complete a quantitative characterization of the effects of the different process parameters. First roughness measurements were made on plasma treated woven fabrics using a Digital Instruments Nanoscope IV atomic force microscope. A loose spring washer rendered the instrument unusable. Although Nylon 6 films were plasma treated by the instrument vendor, it was decided to attempt to use a Zeiss confocal laser scanning microscope for the balance of these initial roughness measurements. Once the roughness values for the films were analyzed, the plasma-treated woven fabrics were analyzed with the LSM; however, the outcome was unsuccessful.

4. Results and Discussion

AFM scans of the woven Spectra fabrics were performed in tapping mode using a tip with a nominal radius of 10 nm. This style of tip had worked well on glass fiber tows to measure the roughness differences among sizing treatments of woven mats. The plasma treatment of the weaves dictated using the full sample and not extracting tows for examination. An image of the weave crest of a single tow captured by the AFM camera at minimum magnification is shown in figure 1.

The measurements were made using only the top-most fibers to avoid any possible interactions between the counter lever and adjacent fibers. The first results appeared to be good, as illustrated in figure 2.

Figure 3 shows the first indications of the camera problem with the AFM. The nature of the problem was unclear at the time and unresolved until a service technician examined the system.

The loose lock washer caused the camera zoom lens to remain at an arbitrary position between full in and full out, producing a false Z value for the interval between tip focus and surface focus. While it was possible to image, the results were nonsensical, e.g., Zµn. It became impossible to engage the tip. The Zeiss confocal laser scanning microscope was used with the nylon film samples until the AFM was repaired.

---

[5] Pappas, D.; Kosik, W.; Bujanda, A.; Demaree, J. D.; Hirvonen, J. K.; Jensen, R.; McKnight, S. Wettability of Nylon Fibers Modified via Atmospheric Plasma Treatment and Surface Roughness. *Proceedings of the 29th Ann. Meeting Adh. Soc.*, Jacksonville, FL, 19–22 February 2006.

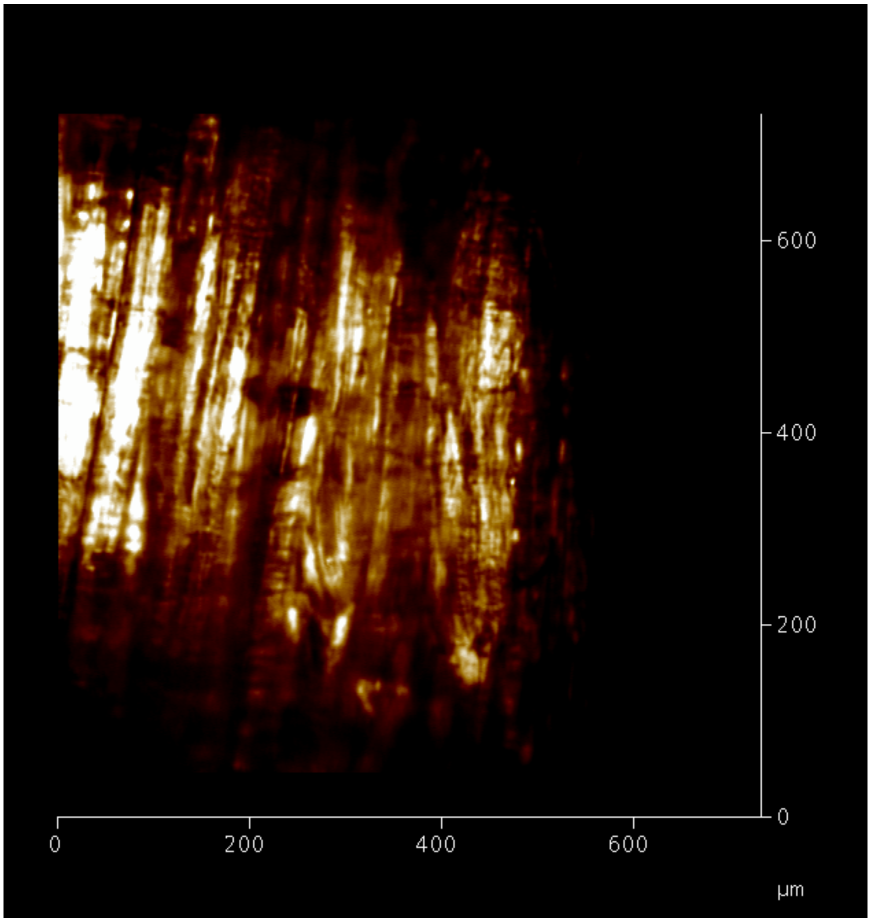

Figure 1. A section of Spectra woven fabric captured by the Nanoscope focusing camera. The camera is zoomed out to allow for rapid searching of the whole weave and for selection and alignment on a single fiber for analysis.

The Zeiss LSM topography module can perform several surface roughness measurements using the image data from a Z-stack. The plasma-treated nylon films and the untreated control sample were examined using 10×, 20×, and 50× objectives and 458-, 514- and 543-nm lasers. The composite in figure 4 illustrates the operation of the LSM topography module. The image at the top is the 10× micrograph of a National Institute for Standards and Technology (NIST) standard reference material (SRM) 2073A sinusoidal roughness standard, Ra = 3.044 ± 0.034 µm. The images immediately below that image are the three-dimensional (3-D) projections of the data.

The first visualization and data set is the calculated roughness using only the “CENTER” function topography correction. The apparent Ra, PSa, equals 4.351 µm. The second has had additional processing; the PSa roughness is 2.988 µm. The SRM data was generated at 10× and 453 nm.

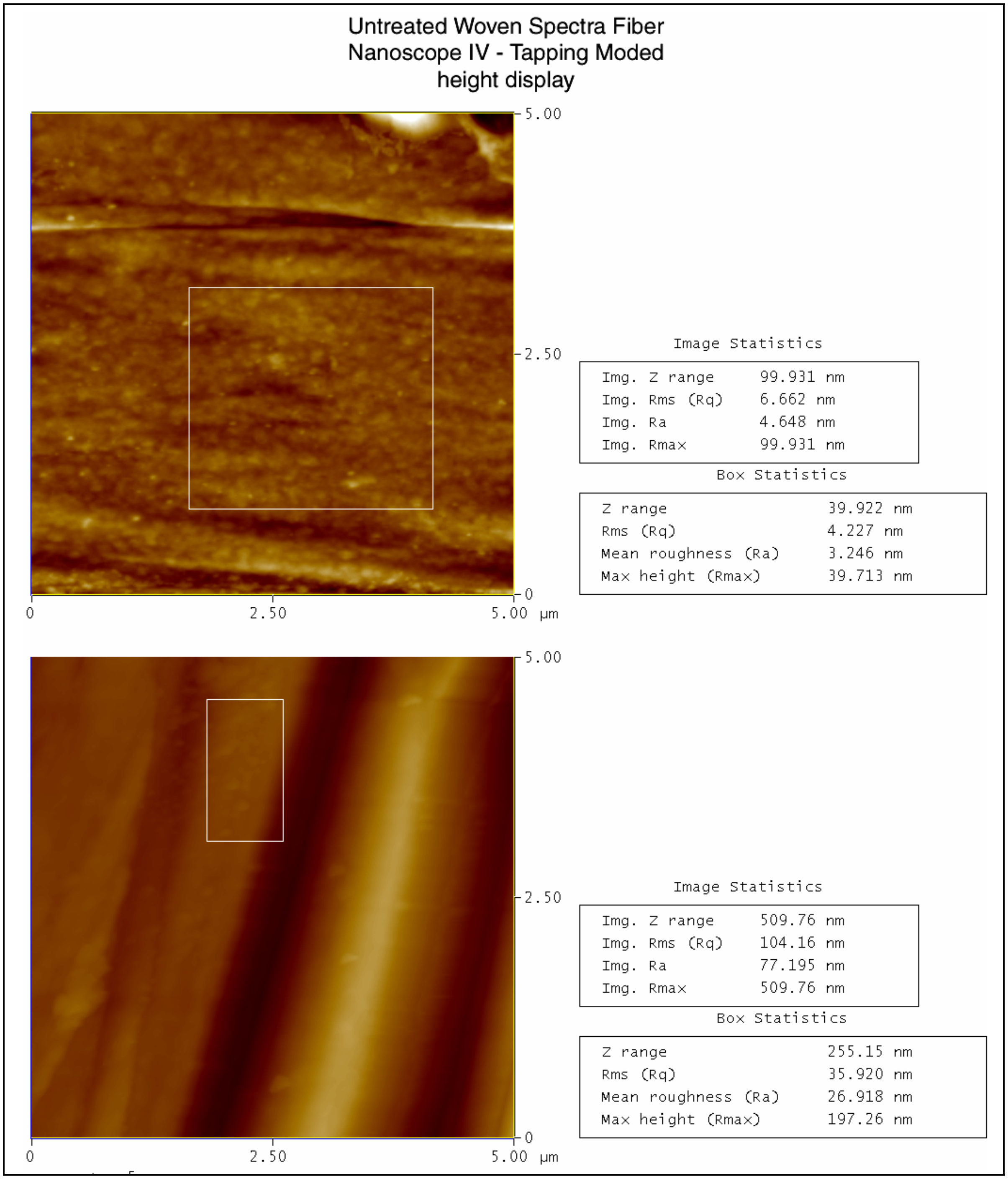

```
Image Statistics
Img. Z range      99.931 nm
Img. Rms (Rq)     6.662 nm
Img. Ra           4.648 nm
Img. Rmax         99.931 nm
Box Statistics
Z range                  39.922 nm
Rms (Rq)                 4.227 nm
Mean roughness (Ra)      3.246 nm
Max height (Rmax)        39.713 nm
```

```
Image Statistics
Img. Z range      509.76 nm
Img. Rms (Rq)     104.16 nm
Img. Ra           77.195 nm
Img. Rmax         509.76 nm
Box Statistics
Z range                  255.15 nm
Rms (Rq)                 35.920 nm
Mean roughness (Ra)      26.918 nm
Max height (Rmax)        197.26 nm
```

Figure 2. Two AFM height micrographs with roughness data of woven Spectra fabric fibers. (The micrographs were collected prior to any known camera issues.)

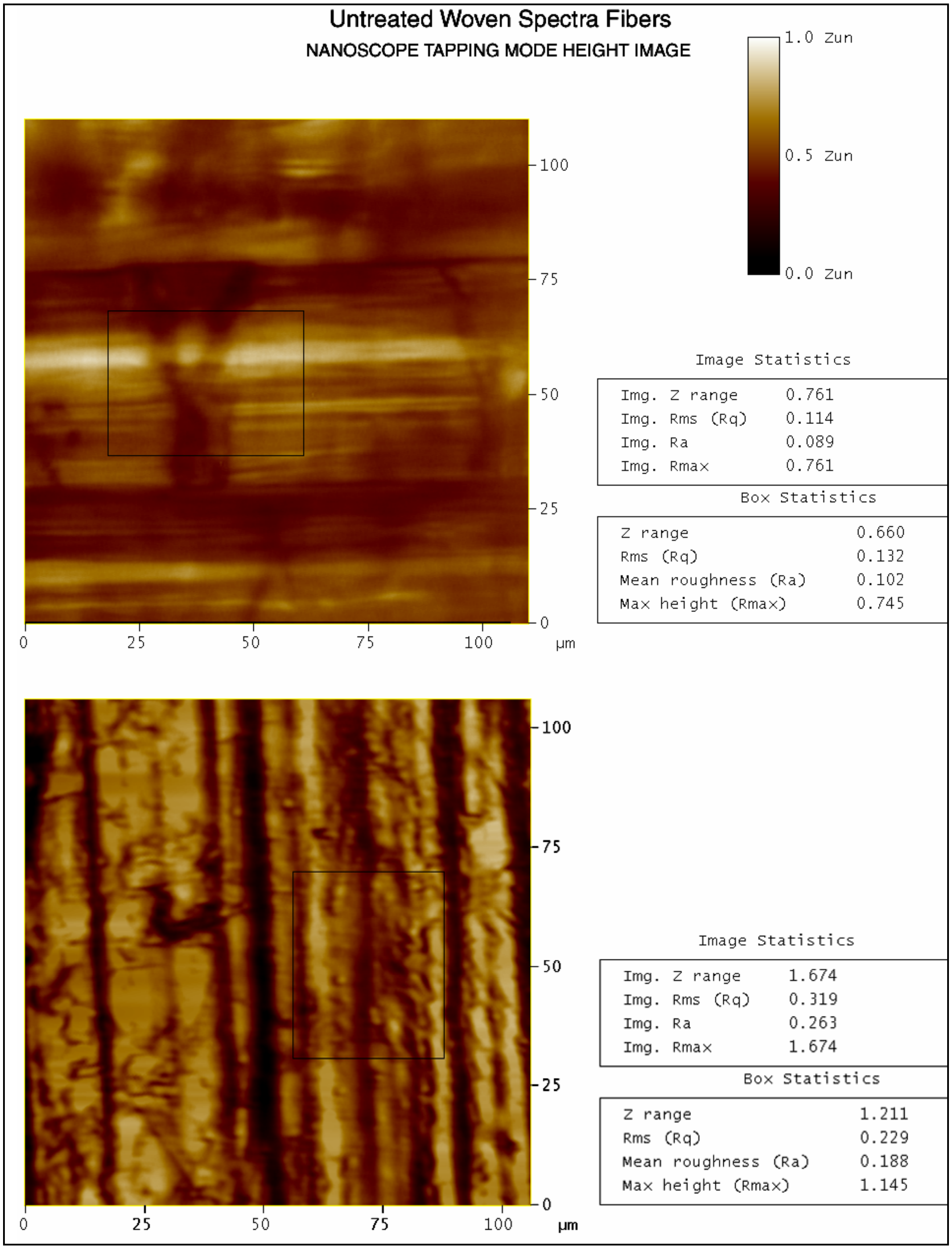

Image Statistics

Img. Z range	0.761
Img. Rms (Rq)	0.114
Img. Ra	0.089
Img. Rmax	0.761

Box Statistics

Z range	0.660
Rms (Rq)	0.132
Mean roughness (Ra)	0.102
Max height (Rmax)	0.745

Image Statistics

Img. Z range	1.674
Img. Rms (Rq)	0.319
Img. Ra	0.263
Img. Rmax	1.674

Box Statistics

Z range	1.211
Rms (Rq)	0.229
Mean roughness (Ra)	0.188
Max height (Rmax)	1.145

Figure 3. Two AFM height micrographs showing the progression of effects caused by the loosening of the camera. The lack of any scale values, shown in the bottom micrograph, was the first indication of a problem. In the top micrograph, the image quality and data analysis are clearly affected.

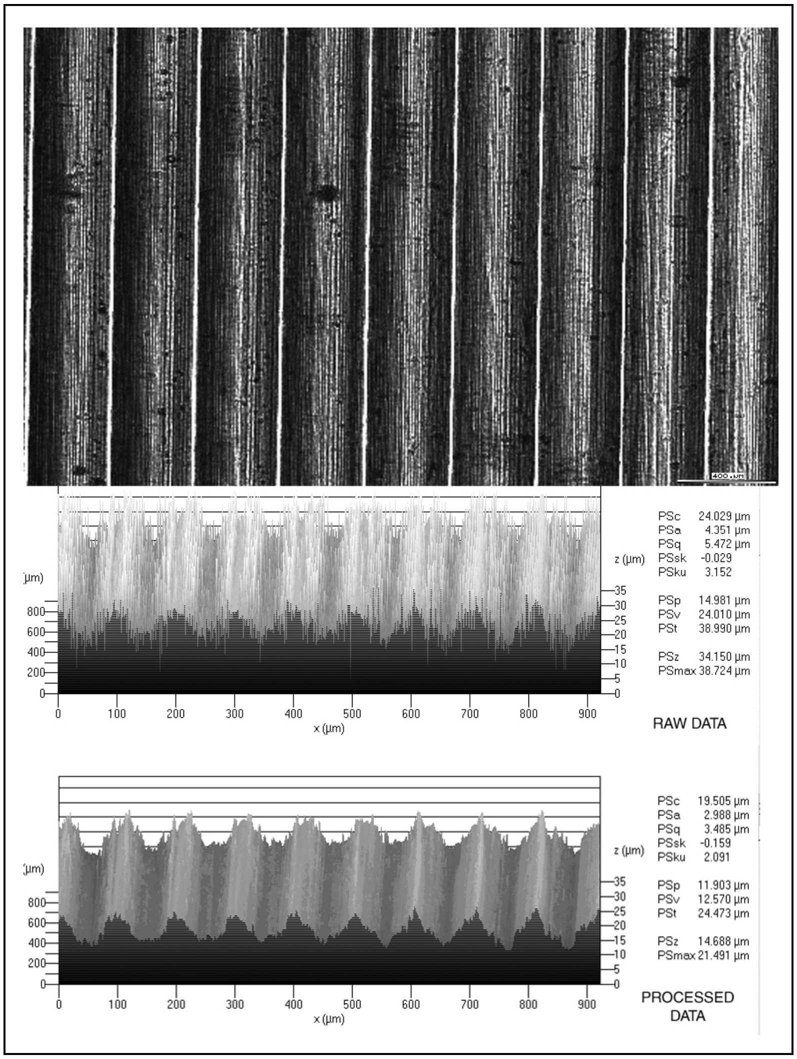

Figure 4. The top image is a two-dimensional (2-D) extended focus of an NIST sinusoidal roughness standard. The lower two images are 3-D visualizations with roughness values of the Z-stack data subjected to two different analysis criteria. The change in parameters affects the appearance of the visualizations and the roughness values.

Based upon the full roughness standards data, table 1 shows inconsistent Nylon 6 film control results and unrealistic roughness values. The magnification vs. roughness relationship was the inverse of previous experiences with the LSM. Initially, the 514-nm laser used was based on having the best low power signal return.

Fastened only at the ends, the film samples in figure 5 bowed. Efforts to use an adhesive covering the entire underside and flatten the specimen were unsuccessful; however, applying the "Cylinder Fit" function in place of the "Plane Fit" corrected the problem.

Table 1. Roughness data initially taken using the confocal LSM system. Only untreated Nylon 6 film was tested. The change in roughness values with increase in magnification mimics trends generally seen with stylist profilometers, but is the inverse of previous experiences.

File No.	Magnification	Z-Stack (µm)	PSc (µm)	PSa (µm)	PSq (µm)	Pin Hole (µm)
Control Nylon 6 Film; 514-ηm Laser						
1	10×	30.10	15.04	0.876	1.131	139.000
2	20×	20.30	10.146	0.537	0.676	84.000
3	50×	6.10	3.032	0.211	0.279	131.000
Average	—	—	9.406	0.541	0.695	—
Standard deviation	—	—	6.038	0.333	0.426	—

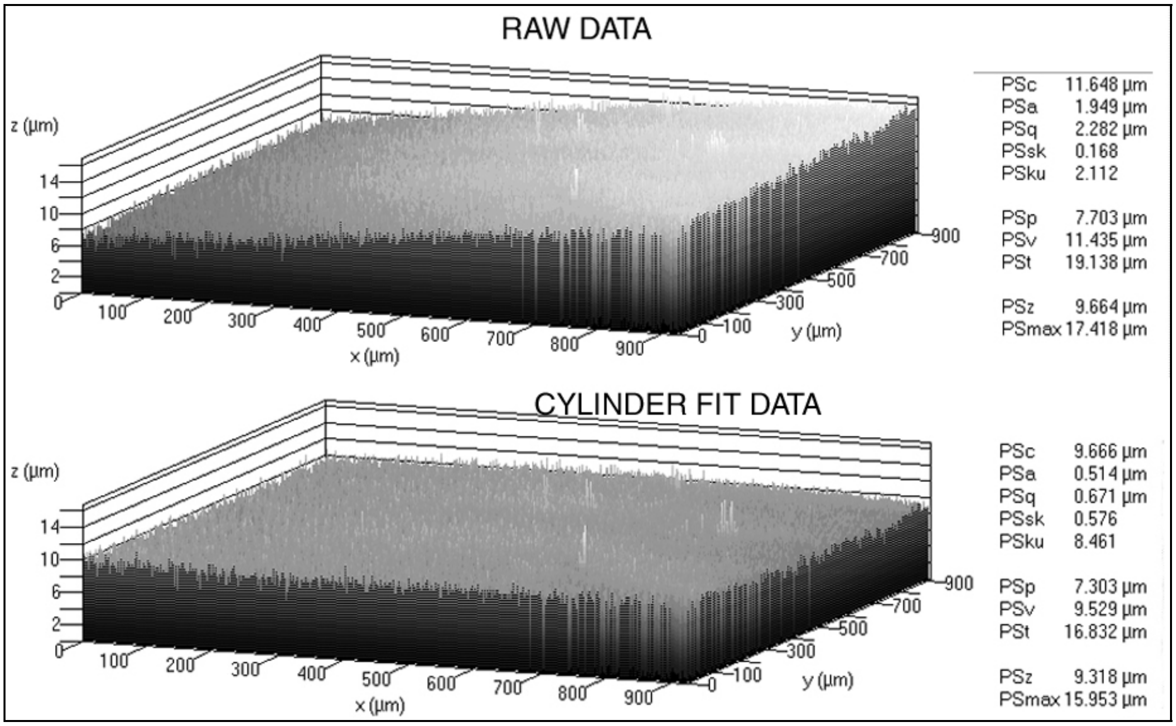

Figure 5. Three-dimensional visualizations illustrating the effects of "plane fitting" on the appearance of those visualizations and the apparent surface roughness of the Nylon 6 film.

The 2-D extended focus surfaces shown in figure 6 contain a series of apparent ridges similar to those of the roughness standard shown earlier. Initially, they were identified as machining scores generated at the time of manufacture, but comparing adjacent areas proved that could not be the case. The specimen has a single orientation for all the Z-stacks collected—how could machine lines change direction? The most probable explanation is that the film bow caused the generation of those ridges. Figure 7 illustrates how the bowing of the nylon film sample would generate the ridge lines.

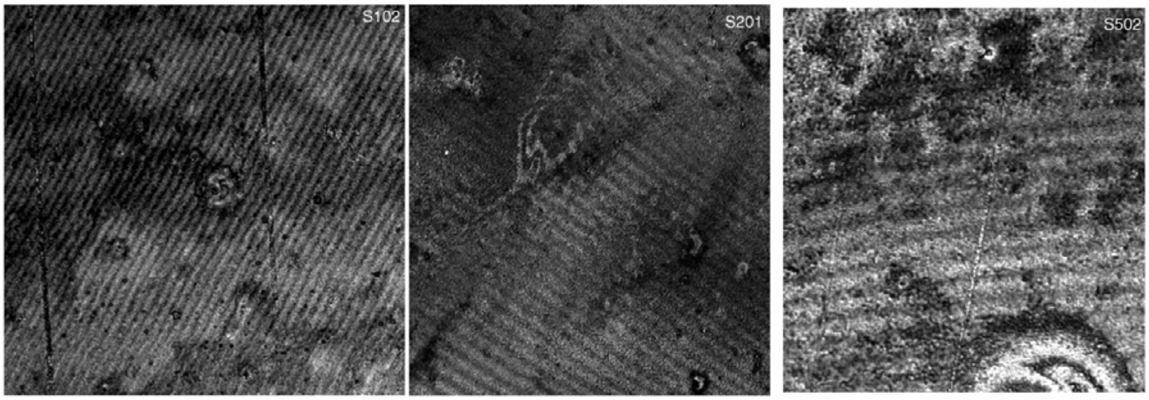

Figure 6. Three 2-D extended focus micrographs taken of nearly adjacent areas of the same Nylon 6 film. Notice that the parallel ridge-like features change direction, size, and radius of curvature from location to location. Because the only repositioning of the sample was done using the x-y stage controls, it is unlikely that those features are real.

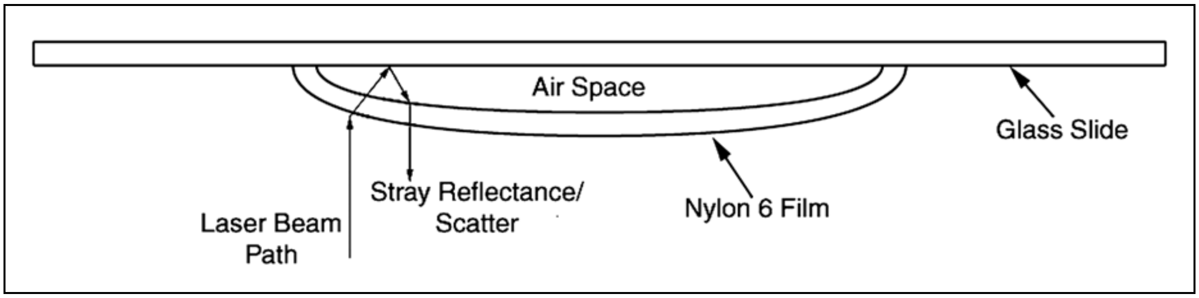

Figure 7. Diagram illustrating the most likely source of the ridge structures presented in figure 6.

Another problem was the slippage or movement of the film during the collection of the Z-stacks. In the 6–13 min it took to generate a stack, the film often slipped lower than the Z interval defined for collection. Because LSM utilizes an inverted microscope, it was not possible to monitor the film or adhesive tape during data generation. Keeping the pinhole equal to 1 airy appeared to minimize any effects on the film roughness measurements.

The 1-airy pinholes did not fully eliminate the laser-generated pseudo ridges, as can be seen in both the 2-D extended focus images, and the data projections or visualizations (figure 8). Any effects from the pseudo ridges on the roughness values appear to have been rendered nominal by using the 1-airy pinholes, as document by the roughness data presented in table 2.

Table 2 shows the roughness values for three different sets of nylon films—the control sample, the plasma treated under He-N_2 plasma, and the plasma treated film with a deposited silicon oxide coating. This data appears to be an accurate reflection of the variation of surface topography.

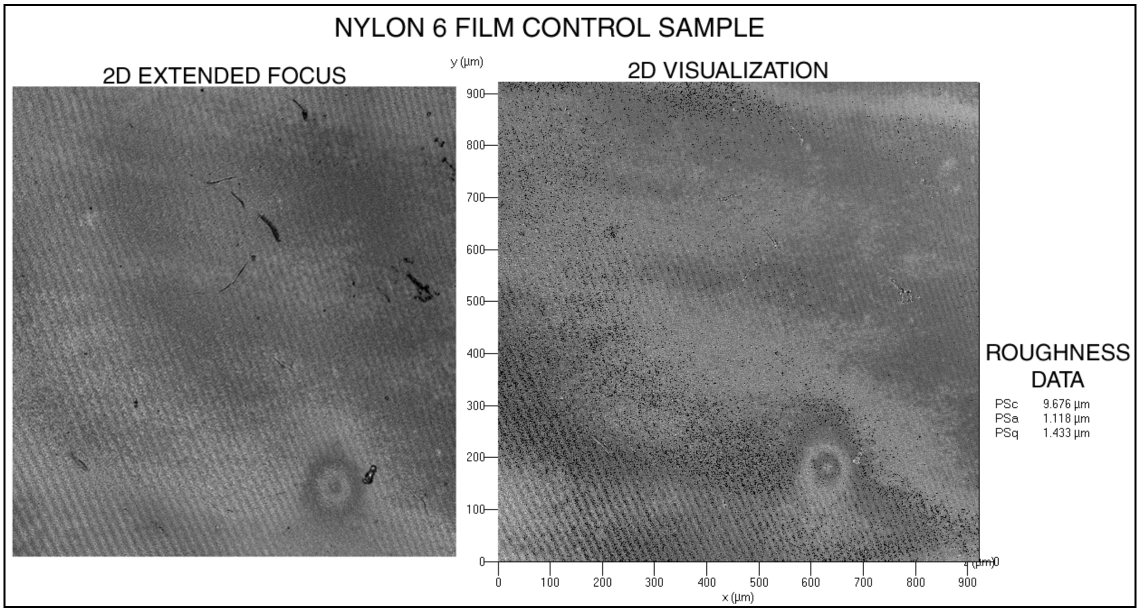

Figure 8. The left image shows a 2-D extended focus micrograph of a Nylon 6 film surface and the right, a 3-D visualization of that same data set. The visualization has been rotated so the Z-axis extends up out of the plane of the paper. The two are similar in appearance but not identical.

We expect an activation process and mild surface etching due to plasma exposure. As the dissociation of molecular nitrogen is unfavorable, it is expected to impose Penning ionization to other molecules present. The role of helium is to remove any surface residing impurities and, through energy transfer mechanisms, cause chain scission and formation of crosslinked layers on the polymer surfaces. Crosslinked layers provide stability to the material and act as a barrier to surface changes.

XPS results reveal that the modified surfaces exhibit a surface rich in oxygen-containing groups. The oxidation was also confirmed by the atomic concentration of oxygen on the surface that increased from 9.88% for the untreated nylon film to 13.49% for the film that was exposed to N_2/He plasma for 4.8 s. The ratio N1s/C1s remained almost constant for all the samples treated under different treatment times. Similar results were observed for Nylon 6 films treated with nitrogen and for low-pressure treatments of polyamide fibers with oxygen plasma. In our case, the O1s/C1s ratio increased from 0.115 for the control film to 0.177 for the nylon film treated for 4.8 s. It is suggested that the plasma treatment induced the formation of carboxylic species on the surface, either in the hydrocarbon or carbonyl groups, which finally enhanced the hydrophilicity of the polymer. The oxygen uptake can be attributed to the presence of atomic oxygen during the process, resulting from the dissociation of atmospheric O_2, and the reaction of the resulting "active" surface obtained after the plasma modification. It is known that the plasma treatment is responsible for chain scission on the polymer surface and thus can react with the environment prior to reaching equilibrium.

Table 2. All the confocal LSM data generated using a 1-airy pinhole and a 10× objective is presented here for comparison, with discussions following. File no. 16 is physically larger than the available ram for the system, which consistently failed to generate any values for this data set.

File No.	**PSc (µm)**	**PSa (µm)**	**PSq (µm)**	**Pin Hole (µm)**
Control 2; 543-ηm Laser				
31	9.676	1.118	1.434	73.000
32	8.992	1.445	1.818	73.000
33	5.889	1.506	1.862	73.000
Average	7.783	1.312	1.648	—
Standard Deviation	2.678	0.274	0.303	—
Treated Nylon 6 Film; 543-ηm Laser				
16	—	—	—	73.000
17	24.130	1.908	2.855	73.000
18	24.141	1.908	2.850	73.000
Average	—	1.908	2.853	—
Standard Deviation	—	0.000	0.004	—
Si-Treated Nylon 6 Film; 543-ηm Laser				
34	5.972	1.481	1.837	73.000
35	1.952	1.545	1.952	73.000
36	26.900	3.041	3.939	73.000
37	27.053	3.635	4.161	73.000
38	57.056	9.838	11.802	73.000
39	8.993	1.479	1.957	73.000
40	8.904	2.305	3.258	73.000
41	44.973	5.893	7.575	73.000
42	59.998	5.980	7.489	73.000
43	44.959	3.194	4.008	73.000
44	38.980	2.416	3.138	73.000
45	35.971	5.115	6.618	73.000
46	15.017	2.545	3.174	73.000
47	32.997	3.472	4.827	73.000
Average	—	3.710	4.695	—
Standard Deviation	—	2.318	2.796	—

Therefore, the observed increased roughness (1.908 µm) after plasma treatment compared to the control sample (1.312 µm) can be attributed to the degradation of the polymer surface and the etching effect due to the presence of atomic oxygen, as the process takes place in open air. The further increase of roughness after the deposition of the silica coating is a proof of the formation of a nonconformal coating on the plasma-treated nylon film. The average roughness is measured to be 3.710 µm, but the standard deviation is 2.318 µm. Therefore, the coating seems to not have the same thickness over the entire area.

The large variation of the silicon-bead plasma treatment roughness data is reflected in the Z-stack visualizations showing a surface transformed to a series of heterogeneous zones by the plasma process. One series of adjacent zones and the accompanying changes in surface roughness is presented in figure 9.

Based upon the LSM roughness results with the films, using the LSM to measure changes in the surface roughness of woven fibers was attempted. The initial raw data appeared promising, as illustrated by the two Z-stack extended focus images in figure 10.

The visualizations in figure 11 show the processed data used for the roughness determinations, which do not approximate the actual surface. The upper left and right visualizations were generated using the same analysis parameters as for the nylon films. The resultant images have significant void areas. Using the "Fill Holes" function in the analysis software corrects the voids problem but generates additional features and changes the roughness data. The obvious solution would have been to crop the stack along the length of any single fiber. The post-processing software only allows a user to define rectangle extraction from the stack without any rotation. Only the capture software allows for rotation during the Z-stack generation process. Attempting to derive an analysis technique using the available functions without the AFM for support appeared to be an open-ended effort. Because the AFM repair was only 2 weeks away, these analyses were not rerun.

5. Conclusion

The objectives for the initial phase of the atmospheric plasma treatment program were to first obtain a practical working understanding of the plasma process parameters. Second was to establish how well our instrumentation could detect, document, and analytically quantify any plasma-induced changes in the materials of interest. Both of these objectives were met, but with varying levels of success.

Nylon fibers and films were plasma treated with nitrogen, helium, and acetylene under atmospheric pressure conditions. Results revealed the improvement of the wettability of the surfaces, accompanied with an increase of their surface tension. The modified materials showed an alteration of their surface composition resulting mainly from the oxygen uptake, as confirmed by XPS analysis. The modified surfaces were rougher and therefore ideal for advanced composite systems requiring enhanced adhesive properties.

The analysis results from the confocal LSM are the reverse of what had been anticipated. The 10× objective produced reliably repeatable data for the nylon film samples. The 50× objective produced imagery clearly documenting plasma-induced changes in the woven fabrics, but could not provide any roughness values. For reasons presented earlier, the accuracy of the confocal LSM roughness values cannot be accepted as reliable as those from an AFM.

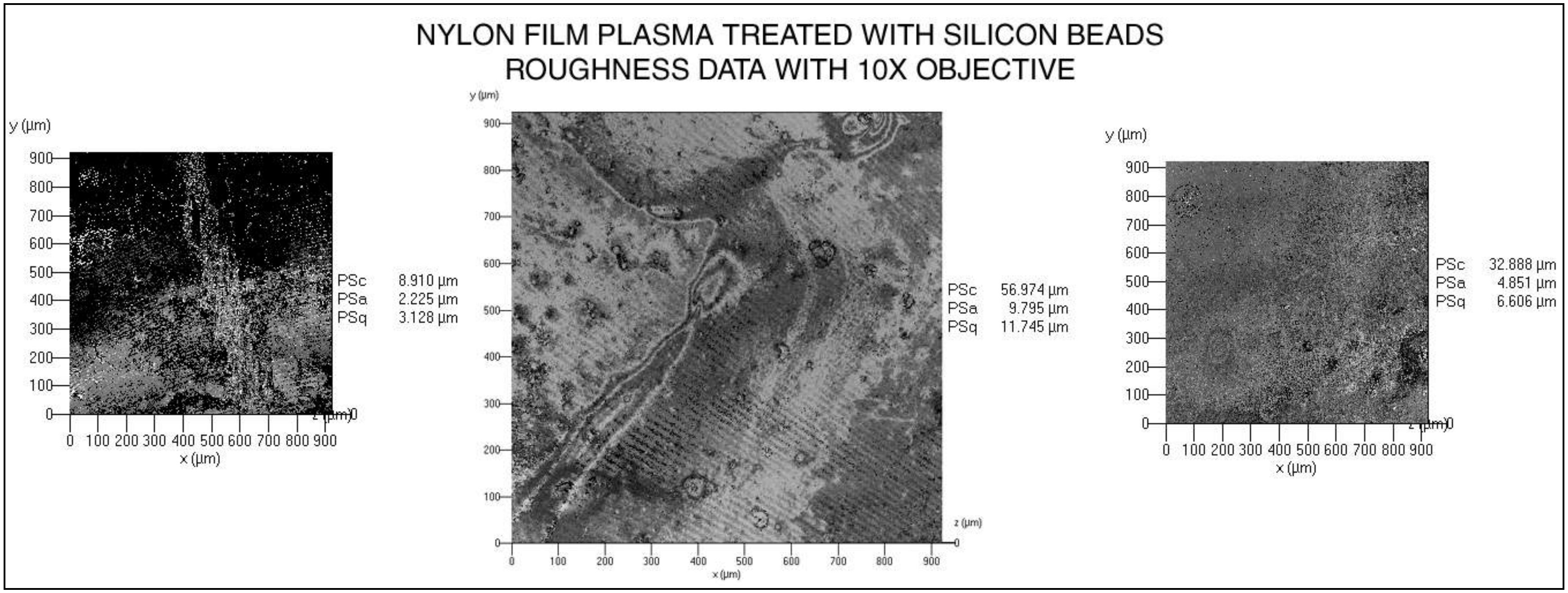

Figure 9. Three extended focus micrographs from the same plasma treated Nylon 6 film, at different locations.

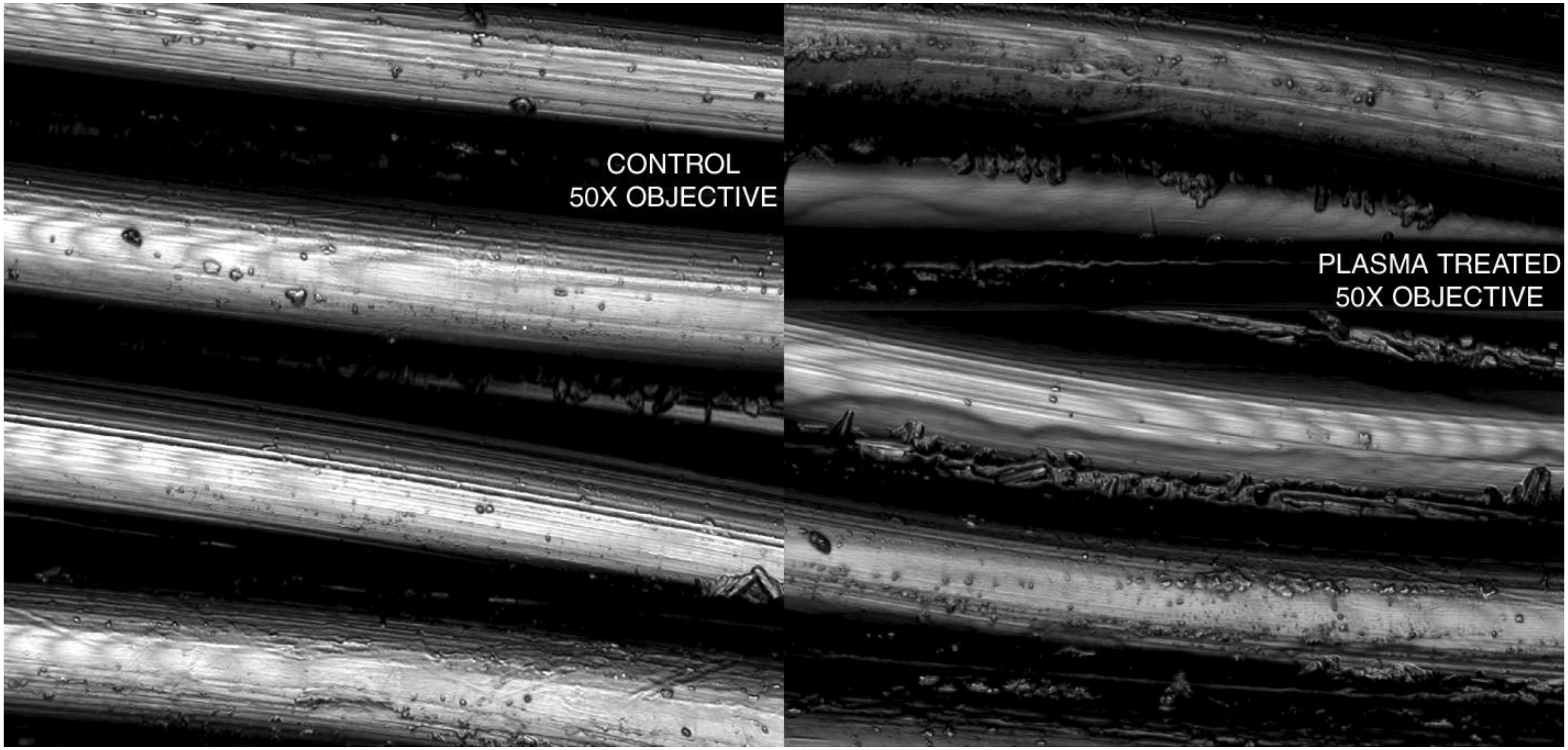

Figure 10. Comparison of the appearances between untreated and treated woven Nylon 6 fabric fibers. The chevron-like features are artifacts from the Z-stack processing. The clarity of the details provided the impetus to attempt using the confocal LSM for roughness measurements of these samples.

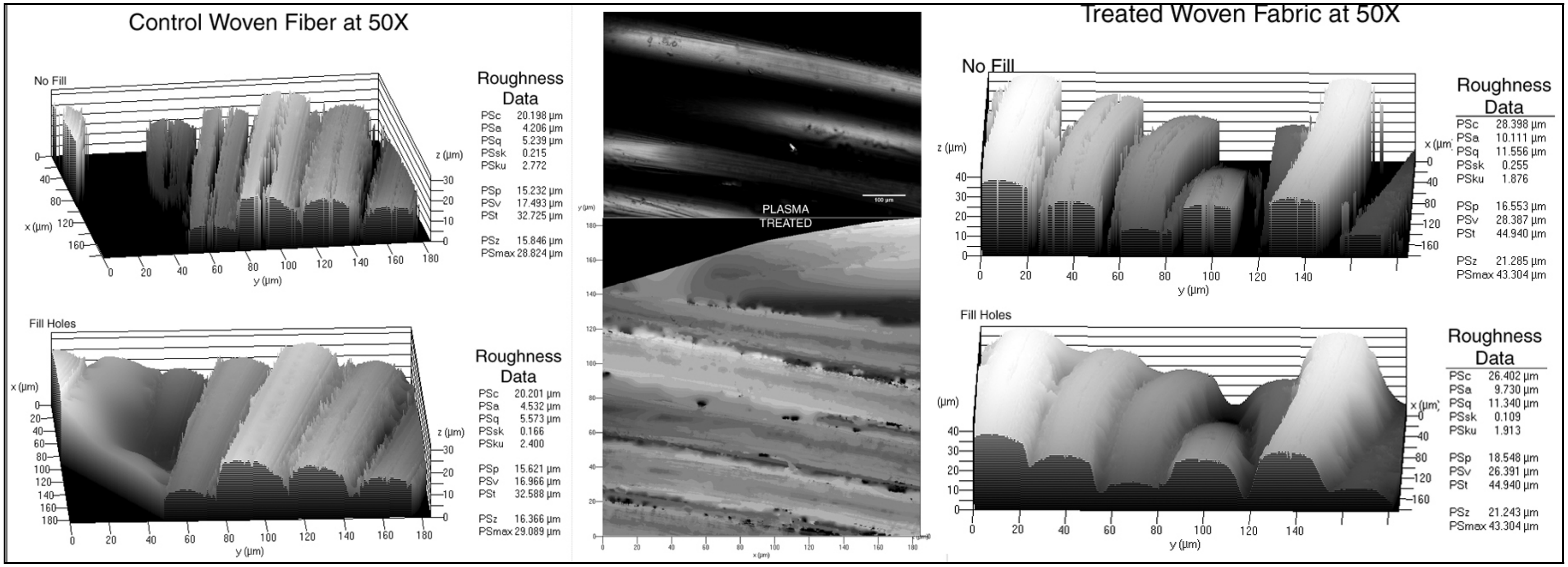

Figure 11. Five 3-D visualizations and the one extended focus micrograph, top center, illustrate one problem with producing roughness values from the fabric Z-stacks, defining a reliable reference plane.

The confocal LSM proved to be the more time efficient of the two methods and thus is better suited to maintain the required time line for testing and analysis. An upgrade of the confocal LSM system will provide a 100× objective; hopefully, this will enable the relative roughness differences of the fabrics to be documented. The AFM will then be reserved for providing more accurate roughness measurement data for a select number of samples.

List of Symbols, Abbreviations, and Acronyms

Roughness

PSc = mean height z.

$$Sc = [1/[Nx * Ny]] * \sum_{i=j}^{Nx} * \sum_{j=1}^{Ny} * z(xi, yj).$$

Psa = arithmetic mean deviation.

$$Sc = [1/[N_x * N_y]] * \sum_{i=1}^{Nx} * \sum_{j=1}^{Ny} * [z(xi, yj) - Sc].$$

PSq = root mean square deviation.

$$Sq = \sqrt{[1/N_x * N_y]] * \sum_{i=1}^{Nx} * \sum_{j=1}^{Ny} * [z(x_i, y_i) - S_c]^2.}$$

Z-stack = a series of micrographs uniformly spaced along Z-axis and stored as a single file.

Airy Unit

$$1_{AU} = \frac{1.22 * \lambda}{NA}.$$

AU = airy unit.

NA = numerical aperture.

λ = wavelength.

NO. OF COPIES	ORGANIZATION
1 (PDF ONLY)	DEFENSE TECHNICAL INFORMATION CTR DTIC OCA 8725 JOHN J KINGMAN RD STE 0944 FORT BELVOIR VA 22060-6218
1	US ARMY RSRCH DEV & ENGRG CMD SYSTEMS OF SYSTEMS INTEGRATION AMSRD SS T 6000 6TH ST STE 100 FORT BELVOIR VA 22060-5608
1	DIRECTOR US ARMY RESEARCH LAB IMNE ALC IMS 2800 POWDER MILL RD ADELPHI MD 20783-1197
3	DIRECTOR US ARMY RESEARCH LAB AMSRD ARL CI OK TL 2800 POWDER MILL RD ADELPHI MD 20783-1197
	ABERDEEN PROVING GROUND
1	DIR USARL AMSRD ARL CI OK TP (BLDG 4600)

NO. OF COPIES	ORGANIZATION
7	DIR USARL AMSRD ARL WM M AMSRD ARL WM MA (6 CPS)

INTENTIONALLY LEFT BLANK.